

Online Fault Detection and Classification of Chemical Process Systems Leveraging Statistical Process Control and Riemannian Geometric Analysis

Alireza Miraliakbar^{1,2}

Fangyuan Ma^{1,3}

Zheyu Jiang^{1*}

¹School of Chemical Engineering, Oklahoma State University, Stillwater, OK, 74078 USA

²Department of Chemical and Biomolecular Engineering, University of Connecticut, Storrs, CT, 06269 USA

³College of Chemical Engineering, Beijing University of Chemical Technology, Beijing, 100029 China

Corresponding author: zjiang@okstate.edu*

Abstract

In this work, we study an integrated fault detection and classification framework called FARM for fast, accurate, and robust online chemical process monitoring. The FARM framework integrates the latest advancements in statistical process control (SPC) for monitoring nonparametric and heterogeneous data streams with novel data analysis approaches based on Riemannian geometry together in a hierarchical framework for online process monitoring. We conduct a systematic evaluation of the FARM monitoring framework using the Tennessee Eastman Process (TEP) dataset. Results show that FARM performs competitively against state-of-the-art process monitoring algorithms by achieving a good balance among fault detection rate (FDR), fault detection speed (FDS), and false alarm rate (FAR). Specifically, FARM achieved an average FDR of 96.97% while also outperforming benchmark methods in successfully detecting hard-to-detect faults that are previously known, including Faults 3, 9 and 15, with FDRs being 97.08%, 96.30% and 95.99%, respectively. In terms of FAR, our FARM framework allows practitioners to customize their choice of FAR, thereby offering great flexibility. Moreover, we report a significant improvement in average fault classification accuracy during online monitoring from 61% to 82% when leveraging Riemannian geometric analysis, and further to 84.5% when incorporating additional features from SPC. This illustrates the synergistic effect of integrating fault detection and classification in a holistic, hierarchical monitoring framework.

Keywords: Process monitoring, Fault detection, Fault classification, Riemannian geometry, Statistical process control

1 Introduction

Enabled by continuous advancements and integration of sensor technologies and digital infrastructure (e.g., the distributed control system), modern chemical plants have been heavily relying on effective and reliable online process monitoring to enhance product quality, reduce operating costs and environmental footprint, and ensure process safety as they continue to expand in scale and complexity Pistikopoulos et al. (2021). Massive arrays of online process data streams, which monitor the plant's equipment performance, manufacturing processes, and mass, energy, and information flows, are continuously produced by numerous sensors and can be leveraged for process monitoring and control Ji and Sun (2022). These online data streams are often nonparametric (i.e., data streams do not necessarily follow any specific distribution) and heterogeneous (i.e., data streams do not necessarily

follow the same distribution), thereby posing challenges to effective chemical process monitoring, such as early fault detection and classification.

Over the past decades, a number of algorithmic methods have been developed to utilize the large volumes of historical and online sensor data for reliable online process monitoring. Among them, dimensionality reduction approaches, such as principal component analysis (PCA) Jackson and Mudholkar (1979) and partial least squares regression (PLS) Geladi and Kowalski (1986); Wold (1966), have received the most attention in the literature Russell et al. (2000); Fezai et al. (2018). While traditional PCA and PLS use linear orthogonal transformations to extract data features, modern chemical processes are typically nonlinear Ma et al. (2023). Thus, nonlinear variations of these methods, such as locally weighted and kernel PCA or PLS Schölkopf et al. (1998); Yin et al. (2017), have been proposed. Nevertheless, these dimensionality reduction-based approaches assume that the statistics used to represent the in-control profiles must also span the subspace defining the out-of-control states William H. Woodall and Gupta (2004). In other words, if one monitors only a few features (e.g., principal components) obtained from historical in-control process data, one should ensure there is not a profile shift in some otherwise undetectable direction during online monitoring. However, in chemical process monitoring, process dynamics can become quite complex and out-of-control states (i.e., process anomalies or faults) cannot be fully enumerated or anticipated a priori. Also, the detection result obtained from these dimensionality reduction-based methods are usually difficult to interpret by operators and process engineers because the features are in the reduced space, which does not have a one-to-one mapping to the original big data sources. In addition, since the number of possible fault scenarios can be quite large, monitoring only the most significant subset of features can cause significant error, as the fault may not be noticeable in the selected features. Furthermore, most existing dimensionality reduction-based methods inherently assume that the full observations of all data streams follow a well-known distribution (e.g., normal distribution). Little work has been undertaken on validating the performance of these dimensionality reduction methods on monitoring nonparametric and heterogeneous online data streams.

More recently, advancements in machine learning (ML) have stimulated the development of various chemical process monitoring algorithms based on supervised methods such as support vector machine Onel et al. (2019); Yin et al. (2014), convolutional neural network, Chengyi Zhang and Wang (2021); Kim et al. (2019) and recurrent neural network Sun et al. (2020); Xavier and de Seixas (2018), as well as unsupervised methods such as autoencoder Zhang and Qiu (2022). Nevertheless, machine learning-based process monitoring techniques still face issues such as overfitting. Also, the process monitoring performance of supervised ML-based methods relies on the availability of a large amount of labeled data, especially faulty data, which are typically limited and hard to acquire in practice. Moreover, ML-based methods do not scale well for new fault scenarios that have not been encountered before.

The limitations of conventional dimensionality reduction and ML-based process monitoring methods motivate us to explore alternative approaches to more effectively conduct fault detection and classification. In terms of alternative methods for fault detection, we have caught attention to latest advancements in statistical process control (SPC) techniques Montgomery (2008). Univariate control charts such as Shewhart chart Shewhart (1930), cumulative sum (CUSUM) Page (1954), and EWMA Roberts (1959) are proven, effective tools that have a solid theoretical foundation and have been extensively studied and used for process monitoring for decades Fu et al. (2017); Khan et al. (2023); Nazir et al. (2019); Sheng-Shu Cheng and Wang (2014); Nawaz et al. (2021). Furthermore, one distinct feature of these SPC techniques is that users can specify their desired false alarm rate (Type I error), thereby offering plant operators the much-needed guarantee and flexibility to safely adjust the alarm sensitivity based on their understanding of the process. Without loss of generality, we choose the CUSUM-based approach as our baseline as these univariate control charts have similar

features. When it comes to modeling several data streams simultaneously, one needs to extend the univariate CUSUM procedure to multivariate ones by first constructing the local statistic for each individual data stream, followed by combining these local statistics together somehow into a single global monitoring statistic. Assuming the local statistic of each data stream follows a normal distribution, Mei (2011) proposed a global monitoring scheme based on the sum of the largest r local statistics. Tartakovsky et al. (2006) proposed using the maximum of local statistics to construct the global monitoring statistic. However, these earlier multivariate CUSUM models are parametric and homogeneous and thus are quite restrictive. And we suspect that these drawbacks have hindered SPC techniques from attracting more attention among industrial practitioners and the process systems engineering (PSE) community.

To address these drawbacks, nonparametric multivariate CUSUM procedures have been recently developed Qiu (2008); Bakir (2006). Most of these nonparametric procedures are based on the idea of monitoring the data stream indices in the ascending-order and descending-order ranklists of data stream measurements at each acquisition time, as it has been shown that these indices can effectively detect process mean shifts or anomalies in downward and upward directions in a nonparametric manner Qiu and Hawkins (2001, 2003). Recently, Ye and Liu (2022) proposed a quantile-based nonparametric CUSUM procedure to monitor heterogeneous processes for the first time, thereby significantly expanding the capability of SPC-based monitoring techniques. Jiang (2023) tested this quantile-based SPC framework on the Tennessee Eastman Process (TEP) benchmark problem Downs and Vogel (1993) and showed that it outperformed existing fault detection algorithms in terms of detection speed. Ma et al. (2024) further incorporated this quantile-based CUSUM procedure Ye and Liu (2022) in a multi-block orthogonal LSTM autoencoder framework and achieved synergistic improvement in fault detection speed and accuracy in the TEP problem compared to state-of-the-art approaches.

In terms of fault classification, a new research direction propelled by Smith et al. (2021) and Smith et al. (2022) is the use of topological data analysis (TDA) and non-Euclidean geometry (e.g., Riemannian geometry) to more effectively extract the fundamental topological and geometric feature underneath the data streams to be analyzed. Specifically, Smith et al. (2022) studied the use of principal geodesic analysis (PGA), a counterpart of PCA applied on the tangent space of the Riemannian manifold, to analyze the TEP dataset and achieved remarkable success in fault classification.

These exciting breakthroughs in fault detection and classification motivate us to develop a holistic process monitoring framework called FARM, which stands for “Fast, Accurate and Robust process Monitoring” in our earlier work Miraliakbar and Jiang (2024) originally presented at the FOCAPD 2024 Conference. As shown in Figure 1, FARM has a hierarchical structure that decomposes process monitoring into fault detection task followed by fault classification task. Each task is conducted by the targeted algorithm. Only if a process fault is detected will the online data be sent for classification. Nevertheless, due to page limit requirement, we were unable to conduct a systematic analysis of the FARM monitoring framework. In particular, questions remain on 1) how well FARM performs in handling the intrinsic trade-off between fault detection speed and accuracy and 2) how well FARM could address the somewhat conflicting objectives between fault detection (“the sooner the better”) and fault classification (whose accuracy improves with increasing time due to larger data size). Although they are clearly important, these aspects have historically been overlooked, as most existing fault classification algorithms use the full-size (spanning ≈ 15 hours) TEP datasets (e.g., Downs and Vogel (1993); Bathelt et al. (2015); Andersen et al. (2022)) for training and testing, posing the question of how these algorithms would perform in online monitoring setting (i.e., with only part of the dataset being available).

To answer these questions, in this work, we conduct a systematic analysis of the FARM framework

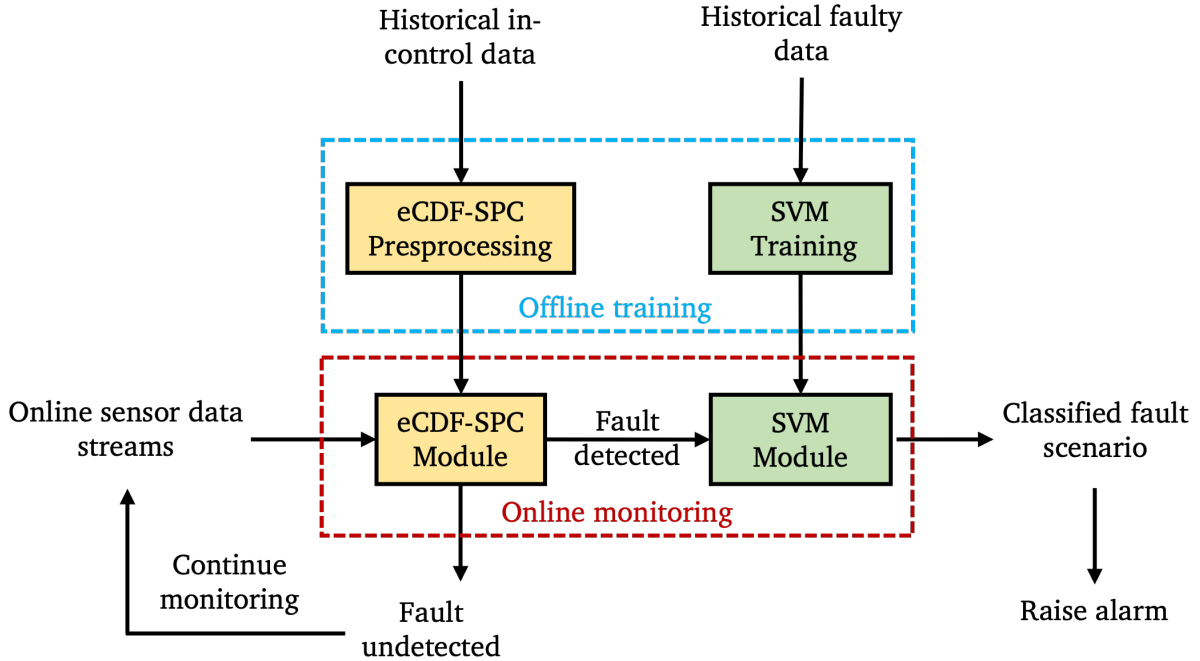


Figure 1: Our FARM framework Miraliakbar and Jiang (2024) for holistic fault detection and diagnosis.

on the TEP benchmark problem as a continuation of our FOCAPD 2024 conference proceeding Miraliakbar and Jiang (2024). For fault detection, we adopt the latest advancement in multivariate nonparametric SPC for generalized heterogeneous process monitoring based on empirical cumulative distribution function (eCDF) estimation Zheng et al. (2024). For fault classification, we present a modified SVM trained by historical faulty data's covariance matrices that are mapped to the tangent space of a Riemannian manifold. We show that our FARM framework achieves competitive performance compared to state-of-the-art methods, especially in detecting widely-known hard-to-detect faults.

2 The FARM Monitoring Framework

2.1 Fault Detection Module

As shown in Figure 1, the FARM framework consists of two distinct modules, one for fault detection and the other for fault classification. In fault detection module, we adopt the state-of-the-art eCDF-based SPC algorithm recently developed by Zheng et al. (2024). Suppose we are monitoring a total of p data streams simultaneously, whose measurements are denoted as $\mathbf{x}(t) = (x_1(t), \dots, x_p(t))$ over the sampling time $t = 1, 2, \dots$, and so on. Here, $x_i(t)$ is assumed to be independently and identically distributed (i.i.d.) across time t for every $i = 1, \dots, p$ during the in-control or out-of-control process. This i.i.d. assumption of data streams is often satisfied when x_{it} are the residual values of data stream measurements Wang and Mei (2015), and has been widely used in monitoring industrial big data streams Changliang Zou and Jiang (2015). First, we construct the local statistic characterization for univariate data stream $x_i(t)$. Let $\mu_i(t)$ be the CDF value of $x_i(t)$ for sensor i at time t . And let $\mathbf{x}_i^0 = (x_{i,1}^0, \dots, x_{i,s_i}^0)$ be a set of historical in-control data from sensor i . Now, consider an online

measurement $x_i(t)$ and compare it with \mathbf{x}_i^0 . From the i.i.d. assumption, the prior distribution of $\mu_i(t)$ is $U(0, 1)$. Furthermore, by defining an indicator function $y_{i,j}(t) = \mathbf{1}(x_{i,j}^0 < x_i(t))$ for every $j = 1, \dots, s_i$, we can track where $x_i(t)$ stands relative to the historical in-control data collected for sensor i . Due to the i.i.d. assumption, the random variable $y_{i,j}(t)$ is also i.i.d. and follows a Bernoulli distribution with respect to the CDF value $\mu_i(t)$:

$$\mathbb{P}(y_{i,j}(t)|\mu_i(t)) \propto [\mu_i(t)]^{y_{i,j}(t)} [1 - \mu_i(t)]^{1-y_{i,j}(t)}. \quad (1)$$

The posterior distribution of $\mu_i(t)$ is given by:

$$\mathbb{P}(\mu_i(t)|y_{i,1}(t), y_{i,2}(t), \dots, y_{i,s_i}(t)) \propto \mathbb{P}(\mu_i(t)) \times \prod_{j=1}^{s_i} \mathbb{P}(y_{i,j}(t)|\mu_i(t)). \quad (2)$$

Noting that $\mathbb{P}(\mu_i(t)) = 1$ and substituting Equation (1) into (2) will give:

$$\mathbb{P}(\mu_i(t)|y_{i,1}(t), y_{i,2}(t), \dots, y_{i,s_i}(t)) \propto [\mu_i(t)]^{\sum_{j=1}^{s_i} y_{i,j}(t)} [1 - \mu_i(t)]^{s_i - \sum_{j=1}^{s_i} y_{i,j}(t)},$$

which corresponds to the probability density function of a Beta distribution with parameters $\sum_{j=1}^{s_i} y_{i,j}(t) + 1$ and $s_i - \sum_{j=1}^{s_i} y_{i,j}(t) + 1$. With this, the CDF value at $x_i(t)$, $\mu_i(t)$, can be readily estimated using the posterior mean of $\text{Beta}(\sum_{j=1}^{s_i} y_{i,j}(t) + 1, s_i - \sum_{j=1}^{s_i} y_{i,j}(t) + 1)$ as:

$$\hat{\mu}_i(t) = \frac{\sum_{j=1}^{s_i} y_{i,j}(t) + 1}{s_i + 2}. \quad (3)$$

Essentially, when the data stream is in control, the CDF value $\mu_i(t)$ follows $U(0, 1)$, whereas when the data stream has a positive (resp. negative) mean shift, $\mu_i(t)$ will approach toward 1 (resp. 0). In other words, the key idea behind the eCDF-based SPC algorithm is to convert the detection of mean shifts in $x_i(t)$ into detecting shifts in the distribution of $\mu_i(t)$ Zheng et al. (2024). Nevertheless, as pointed out by Zheng et al. (2024), directly using the eCDF $\hat{\mu}_i(t)$ for local statistic characterization can pose some implementation challenges, as $\hat{\mu}_i(t) \in (0, 1)$ is not sensitive enough process mean shifts in the distribution of $x_i(t)$. Zheng et al. (2024) proposed to increase the sensitivity by taking log of the $\hat{\mu}_i(t)$ value, thereby resulting in the following one-sided local statistics $W_i^+(t)$ and $W_i^-(t)$ for detecting positive (+) or negative (-) mean shift for sensor i :

$$\begin{aligned} W_i^+(t) &= \max \{W_i^+(t-1) - \log(1 - \hat{\mu}_i(t)) - k, 0\}, \\ W_i^-(t) &= \max \{W_i^-(t-1) - \log(\hat{\mu}_i(t)) - k, 0\}, \quad \forall i = 1, \dots, p; t = 1, 2, \dots, \\ W_i^+(0) &= W_i^-(0) = 0, \end{aligned}$$

where $k > 0$ is an allowance parameter, which restarts the CUSUM procedure if no evidence of mean shift is detected after some time. To detect mean shift in either direction, a two-sided local statistic is defined as:

$$W_i(t) = \max\{W_i^+(t), W_i^-(t)\} \quad \forall i = 1, \dots, p; t = 1, 2, \dots \quad (4)$$

Finally, the top- r approach by Mei (2011) is used to obtain the global statistic for monitoring all data streams. The idea is to rank the two-sided local statistic $W_i(t)$ for all i at every sampling time t from the largest to the smallest, and the global statistics is the summation of the highest r local statistics in the ranklist:

$$V(t) = \sum_{i=1}^r W_{(i)}(t), \quad (5)$$

where (i) corresponds to the index of the i^{th} largest two-sided local statistic. An alarm will be raised when $V(t)$ exceeds a threshold value H , which is determined once an in-control average run length (ARL_0) is set by the operator based on the false alarm rate (FAR). A commonly used ARL_0 is 370, which corresponds to a false alarm rate of no more than 0.0027 (the 3σ limit widely used in quality control Montgomery (2008)). Therefore, this top-r-based stopping criterion not only has concrete theoretical foundation and statistical significance, but also offers great flexibility as operators can customize the choice of H based on the relative severity and tolerance of process failures. An in-depth discussion on the theory and application of this eCDF-based CUSUM procedure can be found in Zheng et al. (2024).

2.2 Fault Classification Module

Once an alarm is raised during online monitoring, the data streams will start to be sent to a modified SVM-based fault classification module that utilizes the covariance matrix derived from $\mathbf{x}(t)$. By this time, although an alarm is raised and operators are alerted, there are typically not enough faulty data to exactly pinpoint which fault the process has. Therefore, to improve the classification accuracy, we introduce a tunable hyperparameter called “patience time” t_p , which corresponds to the number of additional sampling times after the alarm is first raised until the fault is classified. As expected, t_p must be long enough to provide meaningful insights for fault classification module to give accurate prediction, but should not be too long such that the process monitoring framework becomes useless. Once the patience time elapses, FARM would automatically select the process data from the last t_w sampling times called the “window length” for classification. This is not only because the fault classification module can only take a fixed number of samples to construct the covariance matrix, but also to reduce computational costs and mitigate the need to transfer a large amount of data.

To train the SVM model using the historical sensor data corresponding to different fault scenarios, we first compute the covariance matrix of the historical faulty data streams, followed by training the SVM model over the covariance matrix instead of the original faulty data streams. This modification is inspired by the fact that covariance matrices are symmetric and positive definite, and thus always lie on a Riemannian manifold. It has been recently shown that, by respecting this geometric insight, one can greatly enhance the accuracy and interpretability of classification, regression, dimensionality reduction algorithms by conducting these computations on the tangent space of the manifold Smith et al. (2022). Inspired by this result, we map the generated covariance matrices to their tangent space, which intersect the Riemannian manifold where these covariance matrices reside at the geometric mean of the covariance matrices. Through the logarithmic map of Equation (6), the set of covariance matrices of sensor data streams \mathbf{C}_m , which lie on a Riemannian manifold, will be projected onto a tangent space with minimal geometric distortion:

$$\hat{\mathbf{C}}_m = \log_{\bar{\mathbf{C}}}(\mathbf{C}_m) \quad (6)$$

where \mathbf{C}_m , $\bar{\mathbf{C}}$ and $\hat{\mathbf{C}}_m \in \mathbb{R}^{p \times p}$ are covariance matrix of sensor data streams for dataset m , the geometric mean of the set of matrices \mathbf{C}_m and the mapped covariance matrix for dataset m , respectively. After this data preprocessing step, the mapped covariance matrices are used as input features, whereas the corresponding fault scenarios are used as labels to train a standard SVM model using a radial basis function (RBF) kernel.

2.3 Overall Workflow

Here, we summarize the overall workflow for conducting offline training and online monitoring in FARM monitoring framework:

- Offline Training:

1. Historical in-control data of the plant are gathered, normalized and standardized. At this step the means (μ) and standard deviations (σ) of the process variables are stored for later use.
2. For a given set of parameters k , r , and ARL_0 , eCDF-based SPC module is trained to obtain the control limit H , which corresponds to the pre-specified ARL_0 .
3. Historical faulty data of the plant are gathered, normalized and standardized using in-control μ and σ obtained at Step 1.
4. Normalized faulty data are monitored by the eCDF-based SPC. If the global statistics $V(t) \geq H$ at time t , an alarm is raised.
5. Monitored faulty data are gathered and a patience time t_p is chosen as number of samples to gather after the alarm has raised. The choice of t_p depends on the required accuracy.
6. The obtained time series are then preprocessed as only the last time steps with the size of window length t_w is chosen for further analysis. These time series are called “sub-time series” as they are only a subset of the gathered ~~monitored~~ time series.
7. The covariance matrix \mathbf{C}_m of sensor data streams for each sub-time series m is calculated.
8. The covariance matrices are mapped \mathbf{C}_m from the Riemannian manifold to the tangent space to obtain the mapped covariance matrices $\hat{\mathbf{C}}_m$. The mean $\bar{\mathbf{C}}$ is also stored at this stage for online monitoring.
9. The mapped covariance matrices $\hat{\mathbf{C}}_m$ are flattened and used as the features for training the SVM model with the corresponding fault number as the labels.

- Online Monitoring:

1. Online sensor data $\mathbf{x}(t)$ are normalized and standardized using the historical in-control μ and σ obtained during offline training.
2. Normalized online data are monitored by the trained eCDF-SPC module. At time t , if $V(t) \geq H$, an alarm is raised. If not, eCDF-SPC algorithm continues to monitor the process variables.
3. If a fault is detected, the eCDF-SPC algorithm will wait for the set patience time t_p from offline training to gather more faulty data.
4. The last t_w samples are selected prior to covariance calculation.
5. The covariance matrix \mathbf{C} of the selected samples is calculated.
6. The covariance matrix \mathbf{C} is mapped using the obtained mean $\bar{\mathbf{C}}$ from offline training to obtain the mapped covariance matrix $\hat{\mathbf{C}}$.
7. The mapped covariance matrix $\hat{\mathbf{C}}$ is flattened and fed to the trained SVM model in the offline training to obtain the predicted fault label.

3 Case Study: Tennessee Eastman Process

The Tennessee Eastman Process (TEP) is a simulation process developed by the Eastman Chemical Company based on an actual chemical process Downs and Vogel (1993). The TEP has been widely adopted as a benchmark for chemical process control, optimization, and monitoring. As illustrated in the process flow diagram of Figure 2, the TEP contains five major unit operations, which are

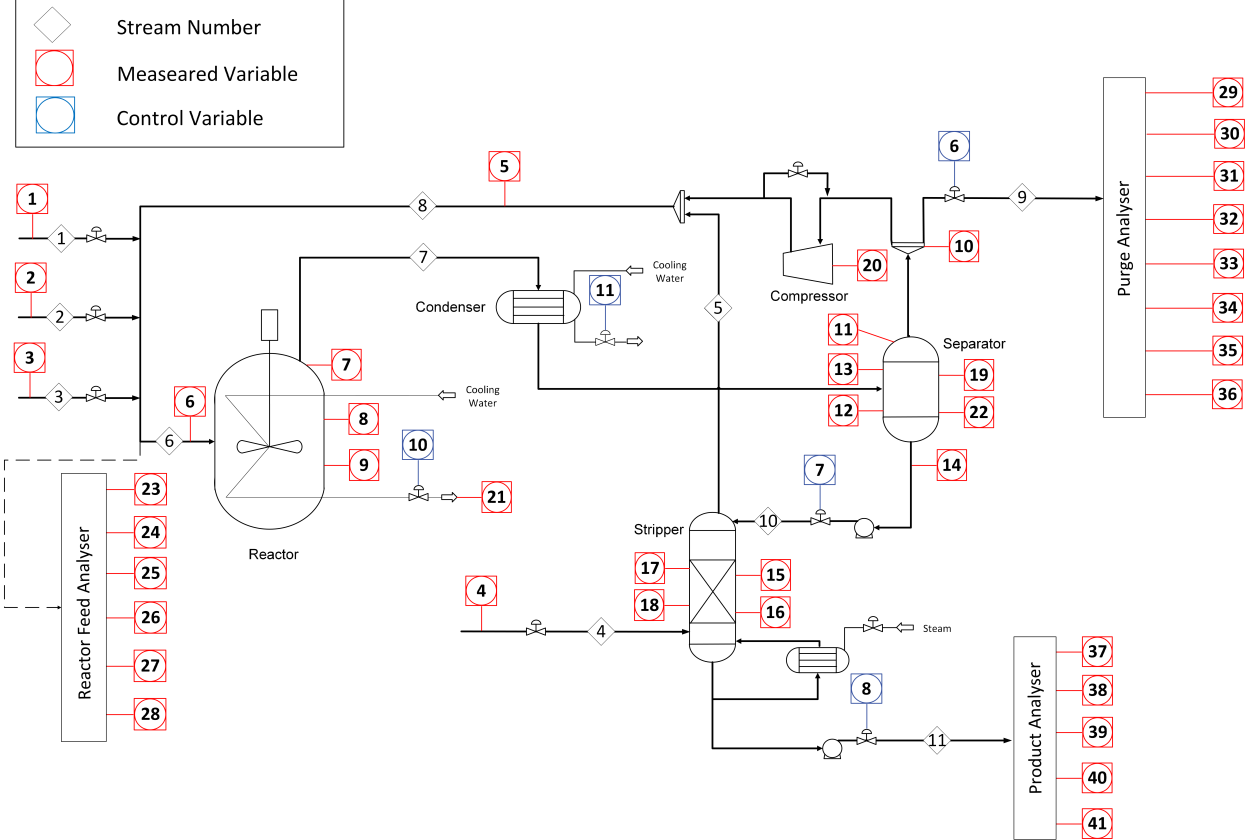


Figure 2: Schematic of Tennessee Eastman Process Downs and Vogel (1993).

associated with 12 manipulated variables and 41 measured variables in total. Table 2 shows the description of each of the 20 faults considered in the TEP problem. For this case study, we synthesize TEP dataset for this case study using the MATLAB/Simulink-based Graphical User Interface (GUI) Andersen et al. (2022). Table 1 lists the variables considered in this study. Six variables are excluded from our analysis since they remain constant in the dataset.

In this study, we evaluate the performance of our FARM framework against four benchmark process monitoring algorithms that we build in house, namely $\text{PCA}-T^2$, Quantile-based SPC (Q-SPC) Jiang (2023); Ye and Liu (2022), Two Class Nonlinear Support Vector Machine (TCNL-SVM) Onel et al. (2019), and Long Short-Term Memory Auto Encoder (LSTM AE) Ren and Ni (2020). These selections cover a spectrum of existing approaches, ranging from dimensionality reduction-based methods, to machine learning-based methods, to SPC-based methods. Three performance metrics, namely fault detection rate (FDR), fault detection speed (FDS), and false alarm rate (FAR), are used to evaluate and compare the performance of different algorithms. The FDR quantifies the model's ability to correctly detect faults when they occur. It is defined as the ratio of the number of correctly identified faulty samples (N_{TP}) to the total number of actual faulty samples ($N_{\text{TP}} + N_{\text{FN}}$). A high FDR indicates that the framework is effective in detecting faults without missing significant events. The FDS, defined as the number of additional sampling times required to detect a fault after it occurs, measures the responsiveness of the model. A lower FDS reflects faster detection. Lastly, the FAR evaluates the framework's ability to minimize false positives, where normal operating conditions are incorrectly flagged as faults. It is defined as the ratio of the number of normal samples misclassified as faulty (N_{FP}) to the total number of normal samples ($N_{\text{TN}} + N_{\text{FP}}$). A low FAR is

critical to ensuring the reliability of the monitoring system and avoiding unnecessary interventions during normal operations. Together, these metrics collectively provide a comprehensive assessment of process monitoring algorithm performance.

Table 1: The detailed information of the monitoring variables used in our case study.

No.	Variable	Description	No.	Variable	Description
1	XMEAS1	A feed	24	XMEAS24	Reactor Feed Composition of B
2	XMEAS2	D feed	25	XMEAS25	Reactor Feed Composition of C
3	XMEAS3	E feed	26	XMEAS26	Reactor Feed Composition of D
4	XMEAS4	A and C feed	27	XMEAS27	Reactor Feed Composition of E
5	XMEAS5	Recycle flow	28	XMEAS28	Reactor Feed Composition of F
6	XMEAS6	Reactor feed rate	29	XMEAS29	Purge composition of A
7	XMEAS7	Reactor pressure	30	XMEAS30	Purge composition of B
8	XMEAS8	Reactor level	31	XMEAS31	Purge composition of C
9	XMEAS9	Reactor temperature	32	XMEAS32	Purge composition of D
10	XMEAS10	Purge rate	33	XMEAS33	Purge composition of E
11	XMEAS11	Product separator temperature	34	XMEAS34	Purge composition of F
12	XMEAS12	Product separator level	35	XMEAS35	Purge composition of G
13	XMEAS13	Product separator pressure	36	XMEAS36	Purge composition of H
14	XMEAS14	Product separator underflow	37	XMEAS37	Product composition of D
15	XMEAS15	Stripper level	38	XMEAS38	Product composition of E
16	XMEAS16	Stripper pressure	39	XMEAS39	Product composition of F
17	XMEAS17	Stripper underflow	40	XMEAS40	Product composition of G
18	XMEAS18	Stripper temperature	41	XMEAS41	Product composition of H
19	XMEAS19	Separator steam flow	42	XMV6	Purge valve
20	XMEAS20	Compressor work	43	XMV7	Separator pot liquid flow
21	XMEAS21	Reactor cooling water outlet temperature	44	XMV8	Stripper liquid product flow
22	XMEAS22	Separator cooling water outlet temperature	45	XMV10	Reactor cooling water valve
23	XMEAS23	Reactor Feed Composition of A	46	XMV11	Condenser cooling water flow

3.1 Fault Detection Performance

To evaluate the fault detection performance, 12000 in-control simulations, each containing 1400 sampling times (sampling frequency is around 10 seconds), are generated using the MATLAB/Simulink GUI Andersen et al. (2022). These in-control simulations are then split into 9600 and 2400 simulations for training and testing, respectively. The threshold value H used in the SPC algorithm is obtained from the 9600 in-control simulations by setting the in-control average run length (ARL_0) to be 500 with $r = 4$ and an optimal allowance parameter of $k = 1.3$. An ARL_0 value of 500 means that, on average, FARM raises 1 false alarm every 500 sampling times when the process is in control (i.e., the average $\text{FAR} = \frac{1}{500} = 0.002$). Under these parameter settings, the threshold value H is determined to be 1546.875. A similar procedure is followed to determine the threshold value corresponding to $\text{ARL}_0 = 500$ for Q-SPC. Table 3 lists the FAR determined from the 2400 simulations in the test set. Both eCDF-based SPC and Q-SPC methods report FAR values that are very close to the originally set value (0.02) in the training set, indicating that the calculated H in the training set is transferrable to testing set. Also, this result highlights the flexibility of SPC-based fault detection algorithms in selecting desired FAR based on operator's preference. On the other hand, TCNL-SVM

Table 2: The detailed information of TEP faults.

Fault No.	Process variable	Type
1	A/C feed ratio, B composition constant (stream 4)	Step
2	B composition, A/C ratio constant (stream 4)	Step
3	D feed temperature (stream 2)	Step
4	Reactor cooling water inlet temperature	Step
5	Condenser cooling water inlet temperature	Step
6	A feed loss (stream 1)	Step
7	C header pressure loss-reduced availability (stream 4)	Step
8	A, B, C feed composition (stream 4)	Random variation
9	D feed temperature (stream 2)	Random variation
10	C feed temperature (stream 4)	Random variation
11	Reactor cooling water inlet temperature	Random variation
12	Condenser cooling water inlet temperature	Random variation
13	Reaction kinetics	Slow drift
14	Reactor cooling water valve	Sticking
15	Condenser cooling water valve	Sticking
16	Variation coefficient of steam supply	Unknown
17	Variation coefficient of reactor heat transfer	Unknown
18	Variation coefficient of condenser heat transfer	Unknown
19	Unknown	Unknown
20	Unknown	Unknown

and LSTM-AE have no control over FAR and the FAR results cannot be transferred between training set and test set, as well as between offline training and online monitoring.

Table 3: Comparison of studied methods in terms of average FAR over 2400 in-control simulations

Model	eCDF-SPC	Q-SPC	PCA- T^2	TCNL-SVM	LSTM AE
FAR	0.0021	0.0025	0.0036	0.1620	0.0086

Next, we conduct 500 out-of-control simulations for each fault with a duration of ≈ 20 hours in the simulation environment (which corresponds to 7000 sampling steps). In Table 4, we summarize the average FDR over 500 out-of-control simulations, from which one can see that our eCDF-based SPC algorithm outperforms benchmark methods in most faults. In particular, it is worth mentioning that eCDF-based SPC algorithm achieves remarkable FDR for detecting Faults 3, 9 and 15, which are incipient faults that are known to be challenging to detect Agarwal et al. (2022). In fact, Q-SPC also performs reasonably well in detecting these three faults, compared to the other methods. The FDR results suggest that SPC algorithms are better at keeping the alarm raised as long as a fault occurs (for theoretical justifications, see Properties 1 and 2 in Zheng et al. (2024)).

Meanwhile, Table 5 summarizes the FDS results for different methods under their respective FARs listed in Table 3. Although SPC-based methods do not perform competitively against other methods, it should be noted that other methods have much higher FAR values. To understand the trade-off between FAR and FDS, we leverage the flexibility of SPC-based methods in specifying any desired FAR and plot the average FDS against the average FAR for eCDF-SPC method in detecting

Table 4: Comparison of the methods in terms of average FDR over 500 out-of-control simulations

Fault number	eCDF-SPC	Q-SPC	PCA- T^2	TCNL-SVM	LSTM AE
1	0.9505	0.9422	0.9808	0.9774	0.9823
2	0.9811	0.9802	0.9761	0.9724	0.9775
3	0.9708	0.9462	0.0282	0.0001	0.0084
4	0.9590	0.9096	0.9997	0.8840	1.0000
5	0.9896	0.9872	0.1519	0.1719	0.0730
6	0.9895	0.9765	1.0000	1.0000	1.0000
7	0.9693	0.9449	1.0000	0.9934	1.0000
8	0.9687	0.9616	0.9528	0.9610	0.9478
9	0.9630	0.8277	0.0197	0.2923	0.0078
10	0.9648	0.9418	0.5158	0.7559	0.6962
11	0.9808	0.9772	0.9868	0.8228	0.9861
12	0.9763	0.9701	0.9601	0.9475	0.9482
13	0.9643	0.9267	0.8932	0.7572	0.8932
14	0.9840	0.9688	0.9864	0.9324	0.9878
15	0.9599	0.4841	0.0115	0.4638	0.0072
16	0.9729	0.9625	0.8317	0.8724	0.8157
17	0.9648	0.9301	0.9060	0.9315	0.9022
18	0.9621	0.8922	0.7052	0.7319	0.7798
19	0.9606	0.4987	0.0120	0.2746	0.0070
20	0.9617	0.9186	0.8441	0.9342	0.8730
Average	0.9697	0.8973	0.6881	0.7338	0.6947

Fault 15. It is clear from Figure 3 that the fault detection speed drastically improves as FAR is relaxed (i.e., increases).

To ensure a fair comparison, we rerun the eCDF-SPC algorithm by specifying the same FAR listed in Table 3 for the three non-SPC methods. From Table 6, it is clear that, under the same FAR, the eCDF-based SPC algorithm outperforms non-SPC methods in terms of FDS in many instances, especially at higher FAR.

3.2 Fault Classification Performance

To prepare the dataset for fault classification, we introduce each fault starting at the 501st sampling time step. Overall, 500 simulations, each containing 500 in-control sampling time steps and 7000 out-of-control sampling time steps, are carried out for each fault, thereby resulting in 10000 simulations in total. 20% of the simulations are used for testing. And each training simulation is monitored by the eCDF-SPC algorithm. As discussed in Section 2.2, as soon as a fault is detected by the eCDF-SPC method, our FARM monitoring framework will wait for t_p sampling time steps to acquire more faulty data. When the patience time is reached, FARM will select the datasets acquired within the last t_w sampling time steps for each simulation to calculate the covariance matrix. Specifically, t_w is set to be the average number of sampling time steps from when the fault is introduced to when classification takes place for all training simulations. By specifying a window length t_w , we mimic process monitoring in real world, where the exact time when a fault occurs is not known to us. Each

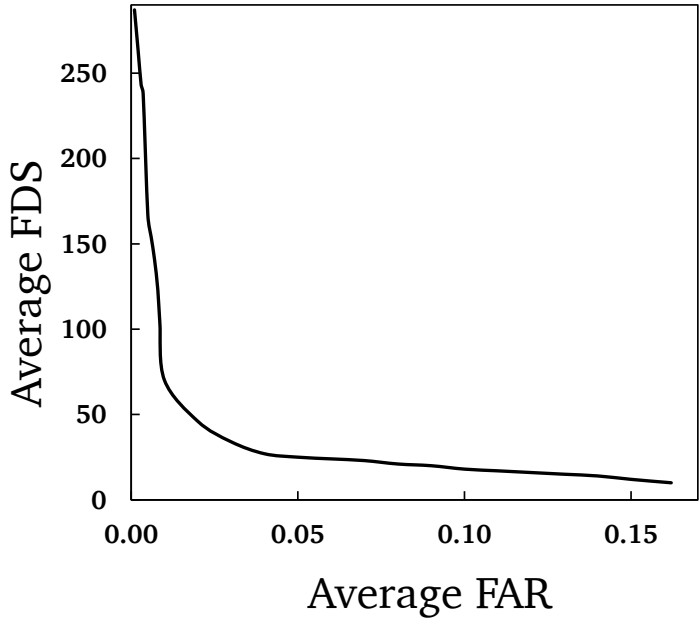


Figure 3: Average FDS versus average FAR for detecting Fault 15 using eCDF-based SPC method.

Table 5: Comparison of the methods in terms of average FDS over 500 out-of-control simulations.

Fault number	eCDF-SPC	Q-SPC	PCA- T^2	TCNL-SVM	LSTM AE
1	82	96	27	37	29
2	127	124	85	87	112
3	202	159	195	34	289
4	69	91	0	1	0
5	73	90	16	13	30
6	69	89	0	0	0
7	65	88	0	3	0
8	215	217	167	70	213
9	251	286	268	98	300
10	240	266	222	67	270
11	136	147	75	143	88
12	166	166	113	87	143
13	236	269	216	171	271
14	114	128	51	89	72
15	263	337	285	53	301
16	192	204	140	81	189
17	237	272	219	95	246
18	234	274	253	100	296
19	257	346	269	24	321
20	255	277	258	45	283
Average	174.6	196.3	142.95	64.9	172.65

Table 6: Comparison of average FDS between eCDF-based SPC algorithm and non-SPC methods under the same FAR.

Fault	FAR = 0.0036		FAR = 0.1620		FAR = 0.0086	
	eCDF-SPC	PCA- T^2	eCDF-SPC	TCNL-SVM	eCDF-SPC	LSTM AE
1	66	27	6	37	45	29
2	106	85	6	87	75	112
3	163	195	8	34	87	289
4	49	0	3	1	33	0
5	51	16	5	13	34	30
6	50	0	4	0	32	0
7	39	0	2	3	23	0
8	142	167	6	70	110	213
9	228	268	7	98	109	300
10	226	222	6	67	109	270
11	127	75	9	143	85	88
12	149	113	7	87	97	143
13	215	216	12	171	106	271
14	109	51	8	89	71	72
15	238	285	10	53	113	301
16	186	140	8	81	100	189
17	192	219	6	95	109	246
18	223	253	5	100	105	296
19	237	269	7	24	108	321
20	230	258	10	45	109	283
Average	151.3	142.95	6.75	64.9	83	172.65

of the covariance matrices will be mapped to the tangent space using Equation (6). Finally, $\hat{\mathbf{C}}_m$ are used as input features to train a SVM model. The model implementation is done in `sklearn` Pedregosa et al. (2011) and hyperparameter tuning is conducted using the grid search method.

To understand how t_p affects fault classification accuracy, we conduct a sensitivity analysis by varying Figure 4 shows the sensitivity analysis performed by varying the patience time from 100 to 4000 sampling time steps and calculating the overall classification accuracy on the test set for all 20 faults. Figure 4, we see that: 1) even if t_p is set to be 0 (i.e., we perform fault classification immediately after an alarm is raised), the overall fault classification accuracy is still more than 50%, 2) the overall fault classification accuracy gradually improves as more patience time is allowed, and 3) there is a diminishing return on the overall classification accuracy when $t_p > 2000$. Based on these results, we set the patience time be 700 (≈ 1.9 hours in simulation environment) for all simulations. And the window length corresponding to $t_p = 700$ is calculated to be $t_w = 873$.

Figure 5 illustrates how Riemannian geometric analysis improves fault classification accuracy. By introducing a data preprocessing step that maps all covariance matrices to a Riemannian manifold, the overall fault classification accuracy is significantly improved from 61% to 82%. For certain faults, such as Fault 19, the relative improvement is greater than 100%. Furthermore, when comparing the confusion matrix of our modified SVM method with a state-of-the-art supervised LSTM AE method

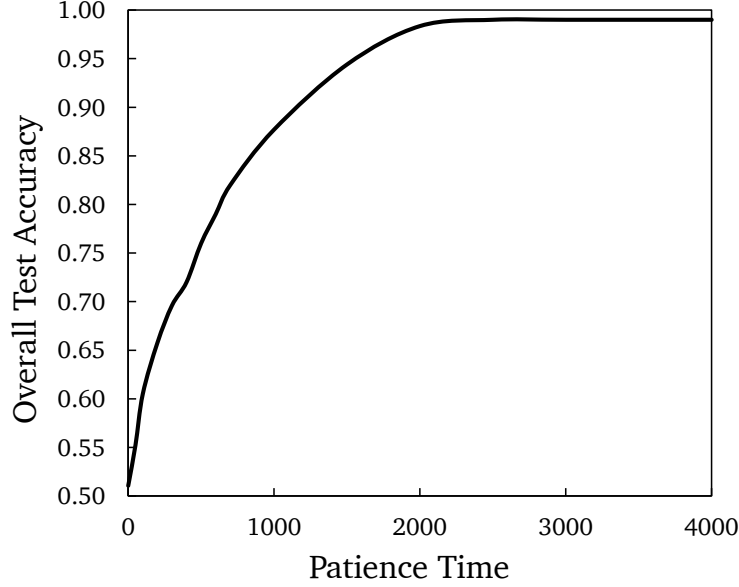


Figure 4: Average fault classification accuracy in the test set for all 20 faults with respect to patience time.

Agarwal et al. (2022), we see that our modified SVM also performs competitively.

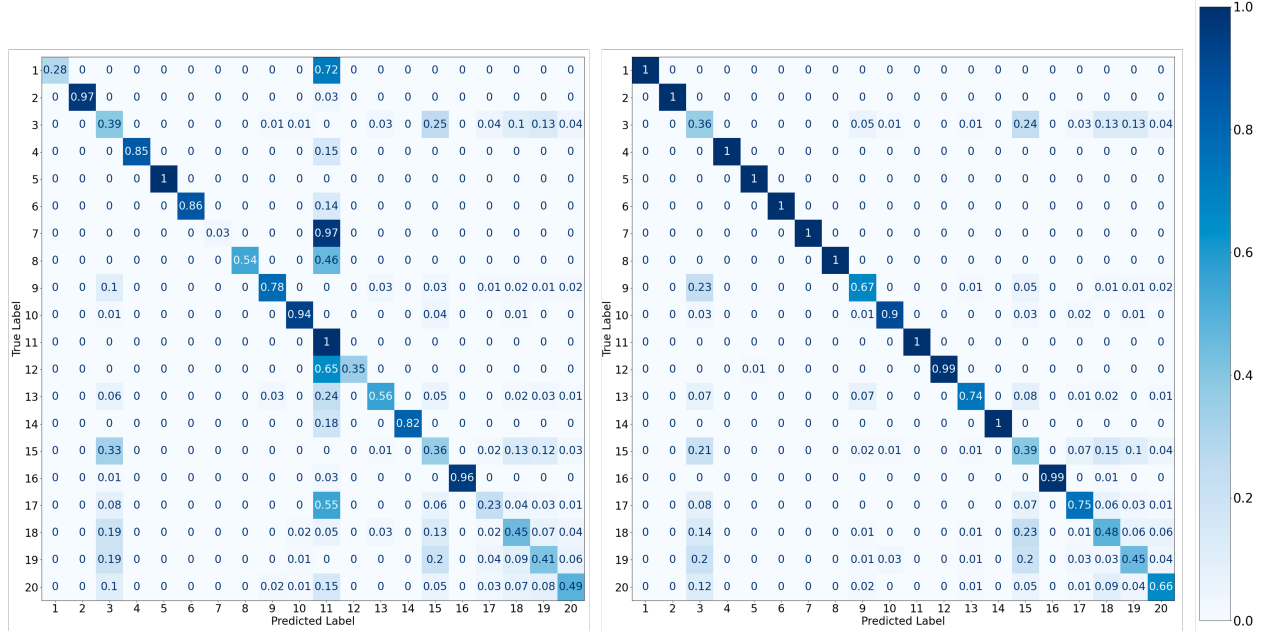


Figure 5: Mapping the covariance matrices to the tangent space improves classification accuracy. (Left): Confusion matrix of SVM method trained on unmapped covariance matrices shows an average fault classification accuracy of 61%; (Right): Confusion matrix of SVM method trained on mapped covariance matrices shows an improved classification accuracy of 82 %. The patience time is set to 700 samples for both cases.

Lastly, to further improve the classification accuracy, we extract the statistical features from

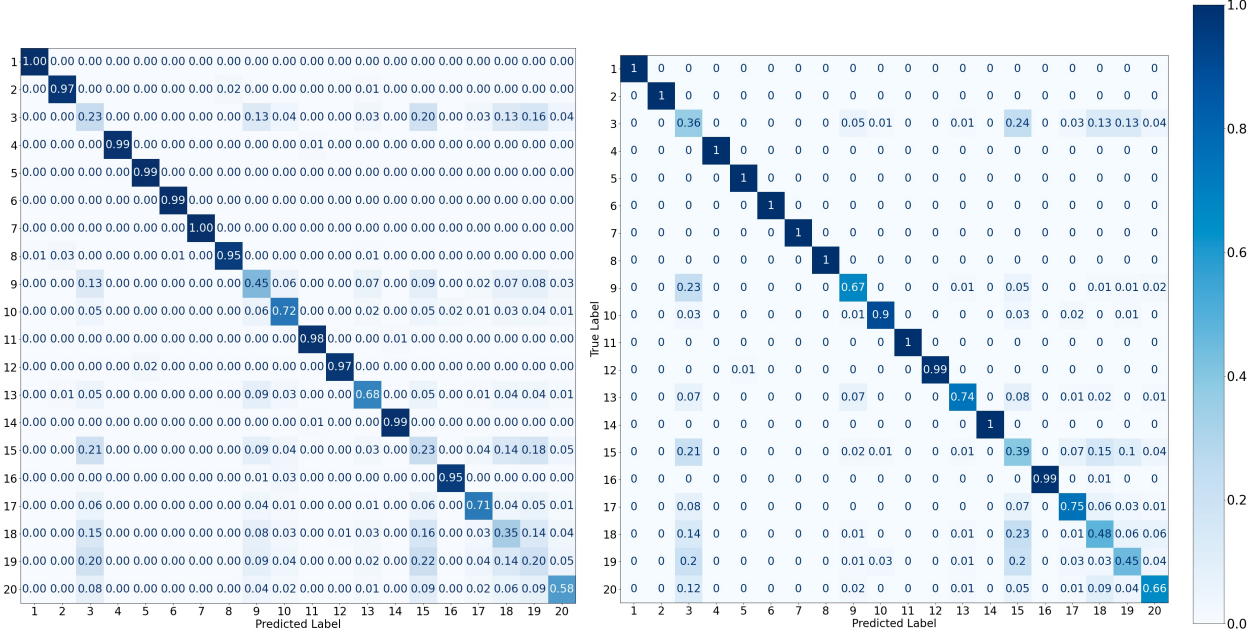


Figure 6: Our modified SVM method outperforms supervised LSTM AE model fault classification accuracy. (Left): The confusion matrix of supervised LSTM AE model with 74% fault detection accuracy; (Right): Confusion matrix of SVM method trained on mapped covariance matrices shows an improved classification accuracy of 82%. The patience time is set to 700 samples for both cases.

global statistic $V(t)$ plot for each simulation. Figure 7 shows an example of the global statistic $V(t)$ plot for Fault 3 in one of simulations. As a proof-of-concept study, we extract key metrics such as mean, standard deviation, median, variance, range, maximum value, number of peaks, and area under the curve (AUC) using `Numpy` Harris et al. (2020) and `SciPy` libraries in Python Virtanen et al. (2020). By incorporating these statistical features obtained from the fault detection module into fault classification, we observe even further improvement in fault classification accuracy from 82% to 84.5% (see confusion matrix in Figure 8), thus demonstrating the synergistic enhancement in process monitoring performance by integrating fault detection and classification in a holistic framework such as FARM.

4 Conclusion

In this study, we enhance our FARM process monitoring framework presented at the FOCAPD 2024 Conference Miraliakbar and Jiang (2024) by introducing the latest advancement in anomaly detection of nonparametric, heterogeneous big data streams using eCDF-based SPC method. Furthermore, our comprehensive case study on the TEP benchmark problem indicates that by this new SPC framework achieves outstanding performance and a good balance among speed, accuracy, and robustness. In terms of fault classification, by introducing basic concepts in Riemannian geometric analysis to well established classification methods, such as the SVM, we observe significant improvement in fault detection accuracy. Furthermore, we show that by incorporating selected statistical features from fault detection module, fault classification performance can be further improved. These promising results open up many exciting opportunities for future research in chemical process monitoring.

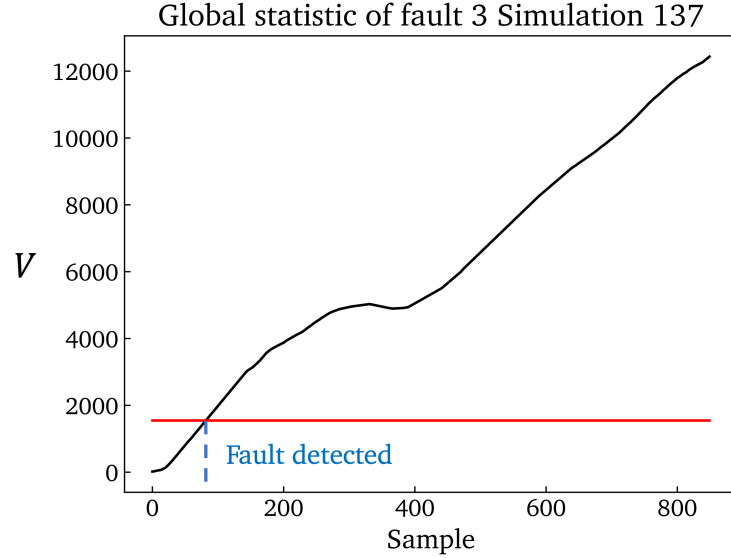


Figure 7: Global statistic ($V(t)$) plot for Fault 3 in one of the simulations with $t_p = 700$. The key features extracted for this plot are mean = 6200.16, standard deviation = 3351.48, median = 5331.36, variance = 11232431.32, range = 12416.88, max = 12436.18, AUC = 5263904.62, and the number of peaks = 3.

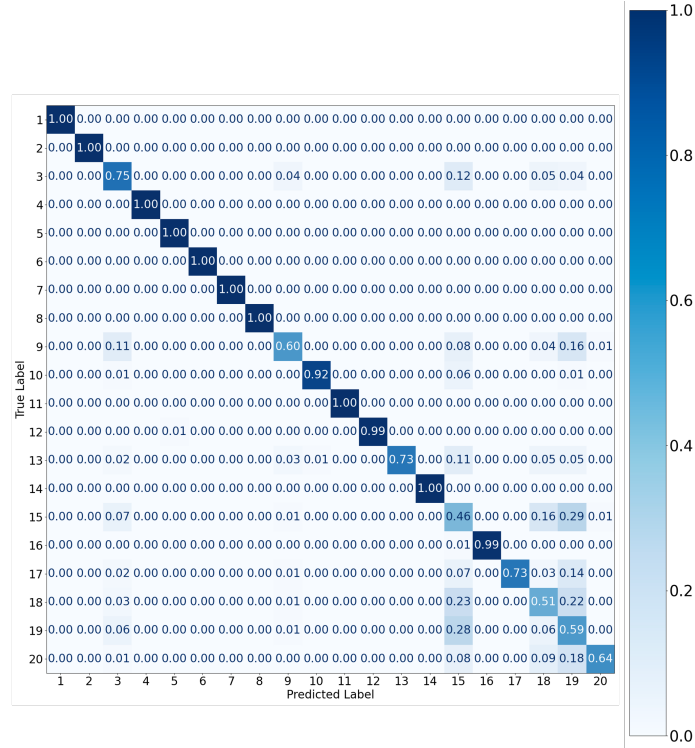


Figure 8: Confusion matrix of modified SVM method shows an improved fault classification accuracy of 84.5% when introducing global statistics features from eCDF-SPC method into the feature set.

Acknowledgments

A.M. and Z.J. acknowledge financial support from U.S. National Science Foundation (NSF) award number 2331080. F.M. and Z.J. acknowledge financial support from Oklahoma Center for Advancement of Science and Technology (OCAST) Oklahoma Applied Research Support (OARS) program grant number AR24-069. Financial support from the startup fund of College of Engineering, Architecture, and Technology at Oklahoma State University is also greatly acknowledged.

References

- Piyush Agarwal, Jorge Ivan Mireles Gonzalez, Ali Elkamel, and Hector Budman. Hierarchical Deep LSTM for Fault Detection and Diagnosis for a Chemical Process. *Processes 2022, Vol. 10, Page 2557*, 10(12):2557, 12 2022. ISSN 2227-9717. doi: 10.3390/PR10122557.
- Emil B. Andersen, Isuru A. Udagama, Krist V. Gernaey, Abdul R. Khan, Christoph Bayer, and Murat Kulahci. An easy to use gui for simulating big data using tennessee eastman process. *Quality and Reliability Engineering International*, 38(1):264–282, 2022. doi: <https://doi.org/10.1002/qre.2975>.
- Saad T. Bakir. Distribution-free quality control charts based on signed-rank-like statistics. *Communications in Statistics - Theory and Methods*, 35(4):743–757, 2006.
- Andreas Bathelt, N. Lawrence Ricker, and Mohieddine Jelali. Revision of the tennessee eastman process model. *IFAC-PapersOnLine*, 48(8):309–314, 2015.
- Xuemin Zi Changliang Zou, Zhaojun Wang and Wei Jiang. An efficient online monitoring method for high-dimensional data streams. *Technometrics*, 57(3):374–387, 2015.
- Jianbo Yu Chengyi Zhang and Shijin Wang. Fault detection and recognition of multivariate process based on feature learning of one-dimensional convolutional neural network and stacked denoised autoencoder. *International Journal of Production Research*, 59(8):2426–2449, 2021.
- J.J. Downs and E.F. Vogel. A plant-wide industrial process control problem. *Computers & Chemical Engineering*, 17(3):245–255, 1993. ISSN 0098-1354. doi: [https://doi.org/10.1016/0098-1354\(93\)80018-I](https://doi.org/10.1016/0098-1354(93)80018-I). URL <https://www.sciencedirect.com/science/article/pii/009813549380018I>. Industrial challenge problems in process control.
- Radhia Fezai, Majdi Mansouri, Okba Taouali, Mohamed Faouzi Harkat, and Nasreddine Bouguila. Online reduced kernel principal component analysis for process monitoring. *Journal of Process Control*, 61:1–11, 2018.
- Xiang Fu, Ran feng Wang, and Zhi yong Dong. Application of a shewhart control chart to monitor clean ash during coal preparation. *International Journal of Mineral Processing*, 158: 45–54, 2017. ISSN 0301-7516. doi: <https://doi.org/10.1016/j.minpro.2016.11.019>. URL <https://www.sciencedirect.com/science/article/pii/S0301751616302514>.
- Paul Geladi and Bruce R. Kowalski. Partial least-squares regression: a tutorial. *Analytica Chimica Acta*, 185:1–17, 1986.
- Charles R. Harris, K. Jarrod Millman, Stéfan J. van der Walt, Ralf Gommers, Pauli Virtanen, David Cournapeau, Eric Wieser, Julian Taylor, Sebastian Berg, Nathaniel J. Smith, Robert Kern, Matti Picus, Stephan Hoyer, Marten H. van Kerkwijk, Matthew Brett, Allan Haldane, Jaime Fernández

del Río, Mark Wiebe, Pearu Peterson, Pierre Gérard-Marchant, Kevin Sheppard, Tyler Reddy, Warren Weckesser, Hameer Abbasi, Christoph Gohlke, and Travis E. Oliphant. Array programming with NumPy. *Nature*, 585(7825):357–362, September 2020. doi: 10.1038/s41586-020-2649-2. URL <https://doi.org/10.1038/s41586-020-2649-2>.

J. Edward Jackson and Govind S. Mudholkar. Control procedures for residuals associated with principal component analysis. *Technometrics*, 21(3):341–349, 1979.

Cheng Ji and Wei Sun. A review on data-driven process monitoring methods: Characterization and mining of industrial data. *Processes*, 10(2), 2022.

Zheyu Jiang. Online monitoring and robust, reliable fault detection of chemical process systems. *Computer Aided Chemical Engineering*, 52:1623–1628, 2023.

Imad Khan, Muhammad Noor-ul Amin, Dost Muhammad Khan, Emad A. A. Ismail, and Wojciech Sumelka. Monitoring of manufacturing process using bayesian ewma control chart under ranked based sampling designs. *Scientific Reports*, 13(1):18240, 2023. doi: 10.1038/s41598-023-45553-x. URL <https://doi.org/10.1038/s41598-023-45553-x>.

Eunji Kim, Sungzoon Cho, Byeongeon Lee, and Myoungsu Cho. Fault detection and diagnosis using self-attentive convolutional neural networks for variable-length sensor data in semiconductor manufacturing. *IEEE Transactions on Semiconductor Manufacturing*, 32(3):302–309, 2019.

Fangyuan Ma, Cheng Ji, Mingyang Xu, Jingde Wang, and Wei Sun. Spatial correlation extraction for chemical process fault detection using image enhancement technique aided convolutional autoencoder. *Chemical Engineering Science*, 278:118900, 2023.

Fangyuan Ma, Cheng Ji, Jingde Wang, Wei Sun, Xun Tang, and Zheyu Jiang. Mola: Enhancing industrial process monitoring using a multi-block orthogonal long short-term memory autoencoder. *Processes*, 12(12), 2024.

Yajun Mei. Quickest detection in censoring sensor networks. In *2011 IEEE International Symposium on Information Theory Proceedings*, pages 2148–2152, 2011.

Alireza Miraliakbar and Zheyu Jiang. Fast, accurate, and robust fault detection and diagnosis of industrial processes. *Systems and Control Transactions*, 3:322–329, July 2024. doi: <https://doi.org/10.69997/sct.108451>.

Douglas C. Montgomery. *Introduction to Statistical Quality Control*. John Wiley & Sons, Hoboken, NJ, 6th edition, 2008. ISBN 978-0-470-16992-6.

Muhammad Nawaz, Abdulhalim Shah Maulud, Haslinda Zabiri, Syed Ali Ammar Taqvi, and Alamin Idris. Improved process monitoring using the cusum and ewma-based multiscale pca fault detection framework. *Chinese Journal of Chemical Engineering*, 29:253–265, 2021. ISSN 1004-9541. doi: <https://doi.org/10.1016/j.cjche.2020.08.035>. URL <https://www.sciencedirect.com/science/article/pii/S1004954120304985>.

Hafiz Zafar Nazir, Tahir Hussain, Noureen Akhtar, Muhammad Abid, and Muhammad Riaz. Robust adaptive exponentially weighted moving average control charts with applications of manufacturing processes. *The International Journal of Advanced Manufacturing Technology*, 105(1):733–748, 2019. doi: 10.1007/s00170-019-04206-y. URL <https://doi.org/10.1007/s00170-019-04206-y>.

Melis Onel, Chris A. Kieslich, and Efstratios N. Pistikopoulos. A nonlinear support vector machine-based feature selection approach for fault detection and diagnosis: Application to the tennessee eastman process. *AIChe Journal*, 65(3):992–1005, 2019.

E.S. Page. Continuous inspection schemes. *Biometrika*, 41(1-2):100–115, June 1954.

F. Pedregosa, G. Varoquaux, A. Gramfort, V. Michel, B. Thirion, O. Grisel, M. Blondel, P. Prettenhofer, R. Weiss, V. Dubourg, J. Vanderplas, A. Passos, D. Cournapeau, M. Brucher, M. Perrot, and E. Duchesnay. Scikit-learn: Machine learning in Python. *Journal of Machine Learning Research*, 12:2825–2830, 2011.

E N Pistikopoulos, Ana Barbosa-Povoa, Jay H Lee, Ruth Misener, Alexander Mitsos, G V Reklaitis, V Venkatasubramanian, Fengqi You, and Rafiqul Gani. Process systems engineering – the generation next? *Computers & Chemical Engineering*, 147:107252, 2021.

Peihua Qiu. Distribution-free multivariate process control based on log-linear modeling. *IIE Transactions*, 40(7):664–677, 2008.

Peihua Qiu and Douglas Hawkins. A rank-based multivariate cusum procedure. *Technometrics*, 43(2):120–132, 2001.

Peihua Qiu and Douglas Hawkins. A nonparametric multivariate cumulative sum procedure for detecting shifts in all directions. *Journal of the Royal Statistical Society: Series D (The Statistician)*, 52(2):151–164, 2003.

Jiayang Ren and Dong Ni. A batch-wise lstm-encoder decoder network for batch process monitoring. *Chemical Engineering Research and Design*, 164:102–112, 2020. ISSN 0263-8762. doi: <https://doi.org/10.1016/j.cherd.2020.09.019>. URL <https://www.sciencedirect.com/science/article/pii/S0263876220304834>.

S. W. Roberts. Control chart tests based on geometric moving averages. *Technometrics*, 1(3):239–250, 1959.

Evan L. Russell, Leo H. Chiang, and Richard D. Braatz. *Data-driven Methods for Fault Detection and Diagnosis in Chemical Processes*. Springer, 2000.

Bernhard Schölkopf, Alexander Smola, and Klaus-Robert Müller. Nonlinear component analysis as a kernel eigenvalue problem. *Neural Computation*, 10(5):1299–1319, 1998. doi: 10.1162/089976698300017467.

Fong-Jung Yu Sheng-Shu Cheng and Steve Hsueh Ming Wang. A cusum control chart to monitor wafer production quality. *Journal of Information and Optimization Sciences*, 35(5-6):483–501, 2014. doi: 10.1080/02522667.2014.943066. URL <https://doi.org/10.1080/02522667.2014.943066>.

W. A. Shewhart. Economic quality control of manufactured product. *Bell System Technical Journal*, 9(2):364–389, 1930.

Alexander Smith, Benjamin Laubach, Ivan Castillo, and Victor M. Zavala. Data analysis using riemannian geometry and applications to chemical engineering. *Computers & Chemical Engineering*, 168:108023, 2022.

Alexander D. Smith, Paweł Dłotko, and Victor M. Zavala. Topological data analysis: Concepts, computation, and applications in chemical engineering. *Computers & Chemical Engineering*, 146:107202, 2021.

Weike Sun, Antonio R.C. Paiva, Peng Xu, Anantha Sundaram, and Richard D. Braatz. Fault detection and identification using bayesian recurrent neural networks. *Computers & Chemical Engineering*, 141:106991, 2020. ISSN 0098-1354.

Alexander G. Tartakovskiy, Boris L. Rozovskii, Rudolf B. Blažek, and Hongjoong Kim. Detection of intrusions in information systems by sequential change-point methods. *Statistical Methodology*, 3 (3):252–293, 2006.

Pauli Virtanen, Ralf Gommers, Travis E. Oliphant, Matt Haberland, Tyler Reddy, David Cournapeau, Evgeni Burovski, Pearu Peterson, Warren Weckesser, Jonathan Bright, Stéfan J. van der Walt, Matthew Brett, Joshua Wilson, K. Jarrod Millman, Nikolay Mayorov, Andrew R. J. Nelson, Eric Jones, Robert Kern, Eric Larson, C J Carey, İlhan Polat, Yu Feng, Eric W. Moore, Jake VanderPlas, Denis Laxalde, Josef Perktold, Robert Cimrman, Ian Henriksen, E. A. Quintero, Charles R. Harris, Anne M. Archibald, Antônio H. Ribeiro, Fabian Pedregosa, Paul van Mulbregt, and SciPy 1.0 Contributors. SciPy 1.0: Fundamental Algorithms for Scientific Computing in Python. *Nature Methods*, 17:261–272, 2020. doi: 10.1038/s41592-019-0686-2.

Yuan Wang and Yajun Mei. Large-scale multi-stream quickest change detection via shrinkage post-change estimation. *IEEE Transactions on Information Theory*, 61(12):6926–6938, 2015.

Douglas C. Montgomery William H. Woodall, Dan J. Spitzner and Shilpa Gupta. Using control charts to monitor process and product quality profiles. *Journal of Quality Technology*, 36(3): 309–320, 2004.

Herman Wold. Estimation of principal components and related models by iterative least squares. In P.R. Krishnaiah, editor, *Multivariate Analysis*, pages 391–420. Academic Press, New York, 1966.

Gilberto M. Xavier and José Manoel de Seixas. Fault detection and diagnosis in a chemical process using long short-term memory recurrent neural network. In *2018 International Joint Conference on Neural Networks (IJCNN)*, pages 1–8, 2018.

Honghan Ye and Kaibo Liu. A generic online nonparametric monitoring and sampling strategy for high-dimensional heterogeneous processes. *IEEE Transactions on Automation Science and Engineering*, 19(3):1503–1516, 2022.

Shen Yin, Xin Gao, Hamid Reza Karimi, and Xiangping Zhu. Study on support vector machine-based fault detection in tennessee eastman process. *Abstract and Applied Analysis*, 2014(1):836895, 2014.

Shen Yin, Xiaochen Xie, and Wei Sun. A nonlinear process monitoring approach with locally weighted learning of available data. *IEEE Transactions on Industrial Electronics*, 64(2):1507–1516, 2017.

Shuyuan Zhang and Tong Qiu. A dynamic-inner convolutional autoencoder for process monitoring. *Computers & Chemical Engineering*, 158:107654, 2022.

Ziqian Zheng, Jiahui Zhang, Lingyun Xiao, Warren Williams, Jing-Ru Cheng, and Kaibo Liu. Online nonparametric process monitoring for iot systems using edge computing. *IISE Transactions*, 0(0): 1–15, 2024.